A Proposed Mechanism for the Reductive Ring Opening of the Cyclodiphosphate MEcPP, a Crucial Transformation in the New DXP/MEP Pathway to Isoprenoids Based on Modeling Studies and Feeding Experiments

Wolfgang Brandt,[a] Marco A. Dessoy,[a] Michael Fulhorst,[a] Wenyun Gao,[b] Meinhart H. Zenk,[b] and Ludger A. Wessjohann*[a]

*Experimental and theoretical investigations concerning the second-to-last step of the DXP/MEP pathway in isoprenoid biosynthesis in plants are reported. The proposed intrinsic or late intermediates 4-oxo-DMAPP (**12**) and 4-hydroxy-DMAPP (**11**) were synthesized in deuterium- or tritium-labeled form according to new protocols especially adapted to work without protection of the diphosphate moiety. When the labeled compounds MEcPP (**7**), **11**, and **12** were applied to chromoplast cultures, aldehyde **12** was not incorporated. This finding is in agreement with a mechanistic and structural model of the responsible enzyme family: a three-dimensional model of the fragment L271 – A375 of the enzyme GcpE of* Streptomyces coelicolor *including NADPH, the Fe_4S_4 cluster, and MEcPP (**7**) as ligand has been developed based on homology modeling techniques. The model has been accepted by the Protein Data Bank (entry code 1OX2). Supported by this model, semiempirical PM3 calculations were performed to analyze the likely catalysis mechanism of the reductive ring opening of MEcPP (**7**), hydroxyl abstraction, and formation of HMBPP (**8**). The mechanism is characterized by a proton transfer (presumably from a conserved arginine 286) to the substrate, accompanied by a ring opening without high energy barriers, followed by the transfer of two electrons delivered from the Fe_4S_4 cluster, and finally proton transfer from a carboxylic acid side chain to the hydroxyl group to be removed from the ligand as water. The proposed mechanism is in agreement with all known experimental findings and the arrangement of the ligand within the enzyme. Thus, a very likely mechanism for the second to last step of the DXP/MEP pathway in isoprenoid biosynthesis in plants is presented. A principally similar mechanism is also expected for the reductive dehydroxylation of HMBPP (**8**) to IPP (**9**) and DMAPP (**10**) in the last step.*

Introduction

Nature's 35 000 or more isoprenoids are biosynthetically formed either through the classical mevalonate pathway (animals, yeast, archaea) or the recently discovered deoxyxylulose phosphate pathway (DXP or MEP pathway: green algae, eubacteria). Most plants possess both pathways.[1–3] The latter metabolic route (Scheme 1), which starts with the synthesis of the first committed intermediate deoxyxylulose phosphate (DXP, **3**), involves a total of seven new enzymes that convert DXP to the common intermediates of both pathways, namely, isopentenyl diphosphate (IPP, **9**) and dimethylallyl diphosphate (DMAPP, **10**).

While the first five genes and enzymes in the metabolic pathway forming and transforming DXP to (2*S*,3*R*)-2,4-dihydroxy-3-methyl-buta-1,3-diylcyclodiphosphate (MEcPP, **7**) are well studied including their reaction mechanisms,[1, 4–10] the last two gene products of the *ispG* (GcpE) and *ispH* (LytB) are functionally less characterized.[2, 3, 11–15] The enzyme GcpE opens the 2,4-cyclic diphosphate **7** with elimination of the hydroxyl group in position 3 and cleavage of the C—O bond at C2 by simultaneous introduction of a 2,3-double bond, thus forming (*E*)-4-hydroxy-3-methylbut-2-enyl diphosphate (HMBPP, **8**). HMBPP itself is subsequently dehydroxylated by the gene product *ispH* (LytB) to form IPP (**9**) and DMAPP (**10**), which involves a third C—O bond cleavage step. The mechanisms of both dehydroxylation steps are a matter of controversy.

The first published mechanistic proposal suggests that the GcpE enzyme catalyzes the reductive opening of MEcPP (**7**) by cleavage of a disulfide bond within the protein and a multiple ionic or radical turnover.[11] The second proposal suggests that GcpE enzyme contains an oxygen-sensitive Fe_4S_4 cluster, which

[a] *Dr. W. Brandt, Dr. M. A. Dessoy, Dr. M. Fulhorst, Prof. Dr. L. A. Wessjohann*
Institute of Plant Biochemistry
Leibniz-Institute, Department of Bioorganic Chemistry
Weinberg 3, 06120 Halle/Saale (Germany)
Fax: (+49) 345-5582-1309
E-mail: wessjohann@ipb-halle.de

[b] *Dr. W. Gao, Prof. Dr. M. H. Zenk*
Biocenter of the Martin-Luther-University Halle-Wittenberg
Weinbergweg 22, 06120 Halle/Saale (Germany)

 DOI: 10.1002/cbic.200300743

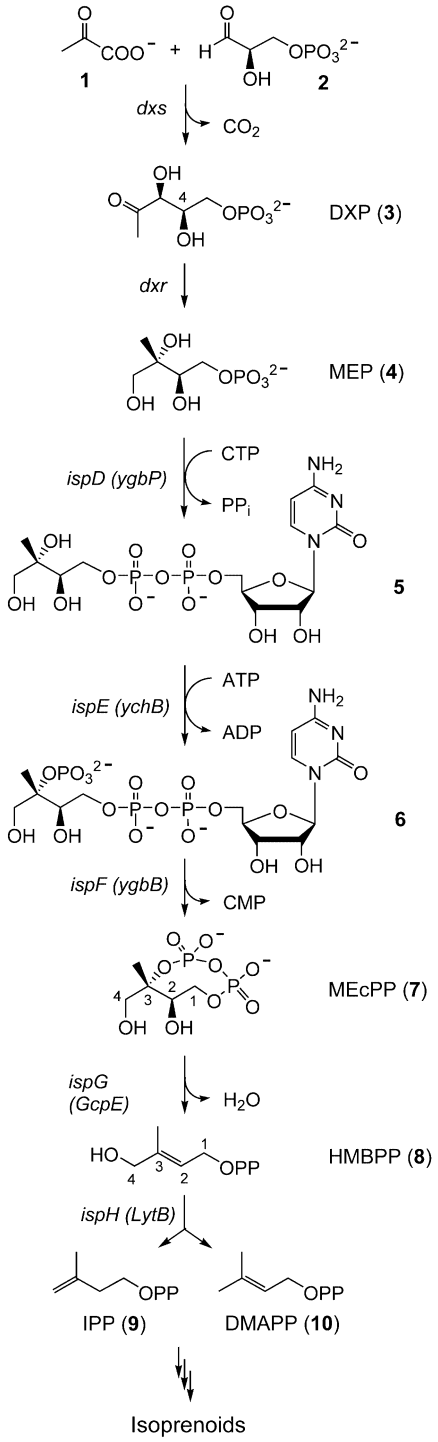

Scheme 1. *Deoxyxylulose phosphate (DXP) pathway for the biosynthesis of terpenoids.*

reductively cleaves the C–O bonds at C2 and C3 of **7**.[12, 15] In both mechanisms, (*E*)-3-methyl-4-oxobut-2-enyl diphosphoric acid (**12**) is proposed as an intermediate (Scheme 2).[3] For the gene product *ispH* (LytB), which catalyzes the last step in the pathway, an Fe–S cluster is again postulated.[14] This cluster is responsible for the two-electron transfer to the substrate and subsequent elimination of the hydroxyl group in position 4, thus leading to a

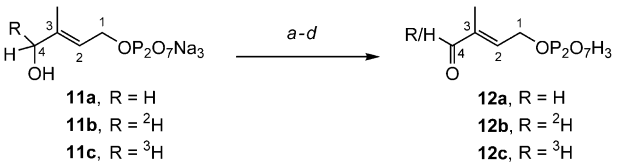

Scheme 2. *Synthesis of (E)-3-methyl-4-oxobut-2-enyl diphosphoric acid (**12a–c**). a) o-Iodoxybenzoic acid (IBX), dimethyl sulfoxide (DMSO), 25 °C, 4 h; b) aq. $NaHCO_3$; c) DEAE Sephadex (formate form); d) Dowex 50 w × 8 resin (H^+ form); ca. 30% overall yield (for **12c**).*

resonance-stabilized allyl cation, which is reduced to the allyl anion and protonated either at carbon 2 or 4 to give IPP or DMAPP, respectively.

We expected that the postulated intermediate aldehyde **12a**, labeled with tritium with high specific activity (**12c**), would allow us to observe the reduction to HMBPP (**8**) and incorporation into terpenoids (mainly phytoene) in the chromoplast system.[1, 4, 16, 17] A successful incorporation would support some of the proposed reactions and help to distinguish between the various mechanisms discussed for the conversion of MEcPP (**7**) to HMBPP (**8**). Note that in all cases NADPH and/or FAD is suggested to act as a cofactor for the reduction of the substrate in the enzymes.

The recently suggested hypothetical mechanism includes two single-electron transfers from an Fe_4S_4 cluster to the substrate with two types of radical intermediates. However, this mechanism does not at all explain what mechanism will cause the ring opening as the initial step of the conversion and if indeed a suggested radical cation may represent a stable intermediate. Knowledge of the enzyme-bound conformation and the detailed conversion mechanism of MEcPP (**7**) to HMBPP (**8**) will be a very helpful prerequisite for the development of specific inhibitors or at least help to derive proposals for further experiments to clarify the mechanism.

Up to now, an X-ray structure of a GcpE protein or any close homologue has not been available. To get a first insight in a three-dimensional structure of this protein, especially of a segment which contains at least a part of the putative active site, we used homology modeling of the amino acid fragment 271–375 of the enzyme of *Streptomyces coelicolor*[18] as an example of a GcpE protein including an Fe_4S_4 cluster. Docking of the substrate will help to determine a likely mechanism for the ring opening of **7**, the elimination of the hydroxyl group, and the formation of HMBPP (**8**). Semiempirical quantum mechanical calculations will help us to understand thermodynamic and kinetic preferences of our suggested mechanism relative to, for example, the hypothetical radical mechanism proposed by Seemann et al. in 2002.[12]

Results

o-Iodoxybenzoic acid (IBX)[19] acts as a versatile oxidizing agent in DMSO and smoothly converts primary and secondary alcohols into the corresponding aldehydes or ketones.[20] Thus, we regarded this procedure as a reasonable basis to try the rather unique conversion of the diphosphorylated diols **11a–c**[17] into

the corresponding aldehydes **12a–c** without special protection procedures. The initially insoluble trisodium salts **11a–c** dissolve upon addition of excess IBX. The diphosphate moiety of **11a–c** (and **12a–c**) is partially protonated, probably owing to the rather acidic oxidant, thus reducing the polarity of the compounds. Although compounds **11a–c** are completely oxidized during the course of the reaction, aldehydes **12b–c** were isolated in only 30% yield. The loss is due to the complex chromatographic purification process. The products are also prone to decompose to the corresponding phosphate esters during the process. Thus, it is important to limit the reaction time to 4 h. Attempts to oxidize **11a–c** with IBX in water failed, although the successful oxidation of ordinary alcohols by IBX in a mixture of acetone/water in the presence of β-cyclodextrin has been reported recently.[21]

It should be noted that the conversion of labeled diphosphates **11b,c** into aldehydes **12b,c** causes the partial loss of the labels contained in the respective starting materials. As a result of primary isotopic effects, the ratio of labeled to unlabeled **12** is not 1.0. The oxidation of deuterated **11b** led to the formation of aldehydes **12b** and **12a** in a ratio close to 1.4, as determined by mass spectrometry. The magnitude of the isotope effect governing the competitive abstraction of H and ^{3}H from **11c** has not been determined. Given that the isotope effect in the latter case is more pronounced than in the former, one can assume that the ratio of **12c** to **12a** is higher than 1.4.

As shown previously, (*E*)-4-hydroxy-3-methylbut-2-enyl diphosphate (**11a**) is a precursor of IPP (**9**), DMAPP (**10**), and various carotenoids when supplied to chromoplasts of *C. annuum*.[17] All other tested intermediates of the alternative pathway entered the chromoplasts and were mainly converted into tetraterpenes. No uptake barrier was observed for these compounds. As shown in Table 1, the incorporation of [4-^{3}H](*E*)-4-hydroxy-3-methylbut-2-enyl diphosphate (**11c**) is in accordance with previous results.[17] Short-term incubation caused the appearance of IPP and DMAPP in a 1:2–1:6 ratio.[22] Smaller amounts of radioactivity were found in the tetraterpene pool, of which the major compound is phytoene. After 6 h incubation, all of the intermediate DMAPP/IPP was consumed; 37% of the supplied radioactivity resides in the tetraterpene pool most of which is phytoene. In contrast, the substitution of [4-^{3}H](*E*)-4-hydroxy-3-methylbut-2-enyl diphosphate (**11c**) by [4-^{3}H](*E*)-3-methyl-4-oxobut-2-enyl diphosphoric acid (**12c**) in the incubation experiments was not successful. The proposed intermediate **12c** is not converted to any of the terpenoid precursors or carotenoids regardless of the incubation time. This indicates that **12** is probably not the expected intermediate.[23]

Also, the isotope dilution technique, supplying chromoplasts with **7**, and after short contact time with chromoplasts and extraction of the labeled material in the presence of unlabeled aldehyde (**12a**) did not indicate the formation of any radioactive product, thus again making the intermediacy of (*E*)-3-methyl-4-oxobut-2-enyl diphosphoric acid (**12a**) unlikely. Supplementation of chromoplasts with labeled MEcPP (**7**) in the presence of the Tzs protein, 6 mM Na-AMP, and 1 mM NADPH led to the incorporation of 20% of the supplied radioactivity into zeatinriboside 5′-phosphate. Supplementation of **12c** for labeled **7** under the same experimental conditions did not give any incorporation of radioactivity, neither of **12c** nor of its reduction product, into zeatinriboside 5′-phosphate.

Based on these results, we conclude that the postulated (*E*)-3-methyl-4-oxobut-2-enyl diphosphoric acid (**12**) is not an intermediate in the alternative terpenoid pathway in higher plants. Of course, the transient intermediacy of **12** concealed within the active site and a concomitant inability of the enzyme to accept **12** directly cannot be ruled out definitely, but seems highly unlikely.

This raises the question of an alternative mechanism. By applying homology modeling, a model of the active site of one example of the GcpE enzyme family was generated and quantum mechanical calculations led to the suggestion of a much more likely new mechanism for the conversion of MEcPP (**7**) to HMBPP (**8**) as discussed below.

Homology modeling of the active site of fragment 271–375 of *Streptomyces coelicolor*

Seemann et al. and Kollas et al.[12, 15] suggested that the GcpE enzymes contain an Fe_4S_4 cluster that mediates the electron transfer to the substrate. To identify the likely active site of the GcpE enzymes and conserved cysteine residues that might act as ligands to the Fe_4S_4 cluster, a multiple alignment of all known sequences of the GcpE family was performed. Figure 1 shows the most important fragments resulting from this alignment. It is evident that only three cysteine residues (C281, C284, and C316) are 100% conserved. These may participate in binding the Fe_4S_4 cluster. Furthermore, an arginine (R286), an asparagine (N319), and a glutamate (E323) are also conserved 100% among other residues. Seventyeight X-ray structures of enzymes containing such a cluster (see Brookhaven Protein Data Bank)[24] are known. The Fe_4S_4 cluster is covalently bound either by four cysteine residues or by only three cysteines.

Table 1. *Incubation of [4-^{3}H](E)-4-hydroxy-3-methylbut-2-enyl diphosphate (**11c**) and [4-^{3}H](E)-3-methyl-4-oxobut-2-enyl trihydrogen diphosphate (**12c**) with chromoplasts of* C. annuum *and subsequent analysis of potential reaction products [% of radioactivity].*

Substrate	*t* [min]	IPP (**9**)	DMAPP (**10**)	Tetraterpene fraction	Phytoene
[4-^{3}H](*E*)-4-hydroxy-3-methylbut-2-enyl diphosphate (**11c**)	10	18.2	17.1	12.3	36
	360	0	0	37.3	50
[4-^{3}H](*E*)-3-methyl-4-oxobut-2-enyl trihydrogen diphosphate (**12c**)	10	0	0	1.0[a]	0
	360	0	0	5.4[a]	0

[a] As dephosphorylated (*E*)-3-methyl-4-oxobut-2-enyl trihydrogen diphosphate (**12**).

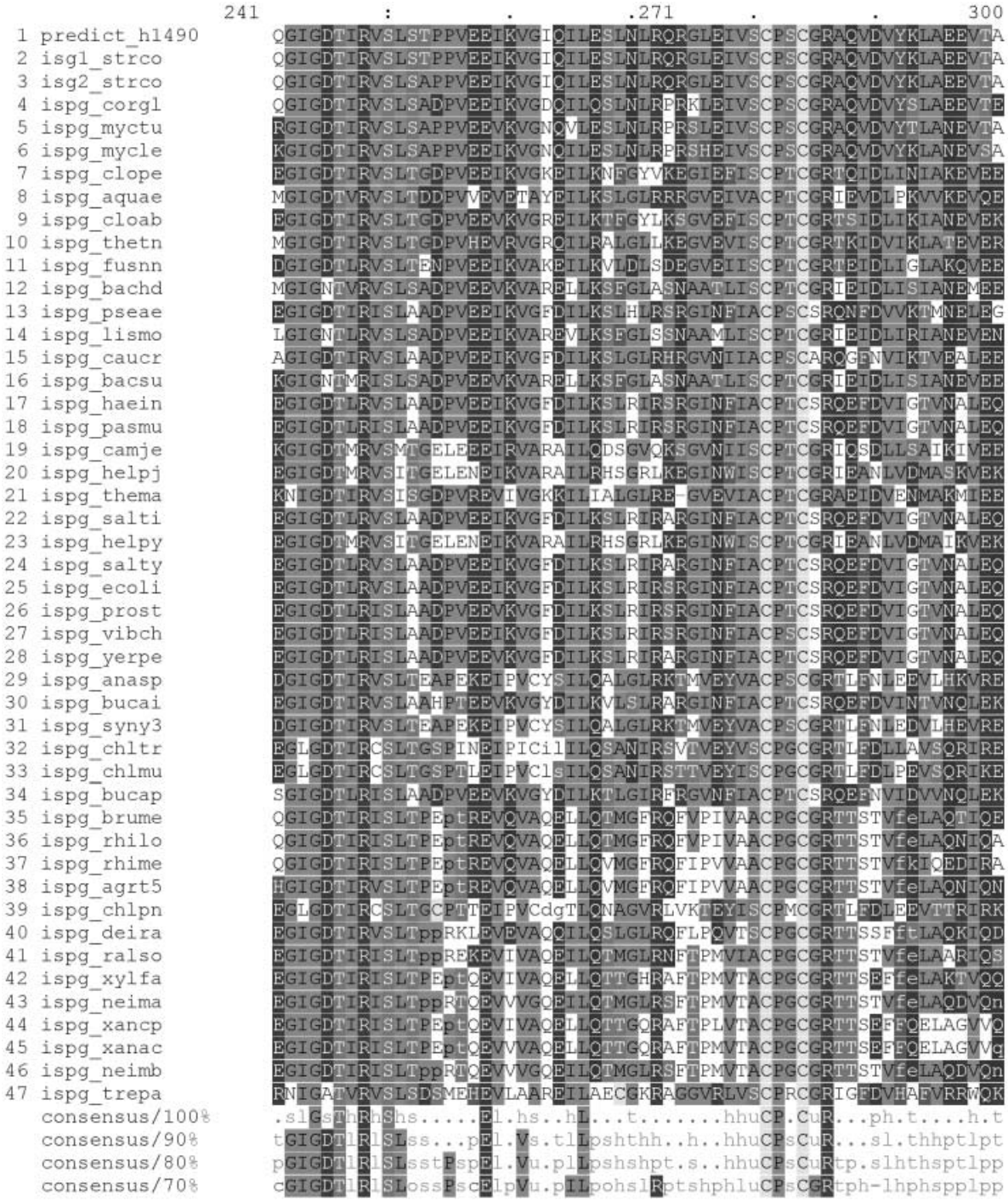

Figure 1. *Partial alignment of fragments 241 – 360 of all enzymes belonging to the GcpE family. Percentage of consensus residues are listed in the lower four rows.*

Next, we tried to generate a three-dimensional model of one of the GcpE proteins. An initial search for sufficient homology for the complete sequence of GcpE for proteins with known X-ray structures using the 3d-pssm server[25, 26] gave no useful results. The homology to any other protein was not high enough. Subsequently we shortened the sequence stepwise and again performed searches for homologous proteins. Finally, fragment L271 – A375 of GcpE of *Streptomyces coelicolor* (Swissprot: Q9X7W2)[18] gave a sequence identity score of 25 % and a PSSM-E-value of 1.66×10^{-8} homology with a sulfite reductase of *Escherichia coli* (pdb: 1AOP).[27] With a certainty of 95 %, the latter enzyme was judged useful for homology modeling of the GcpE protein. The alignment of both sequences is shown in Figure 2.

Based on this alignment, we created a model of the likely active site of GcpE with bound Fe_4S_4 cluster by using the homology modeling tool in MOE (molecular operating environ-

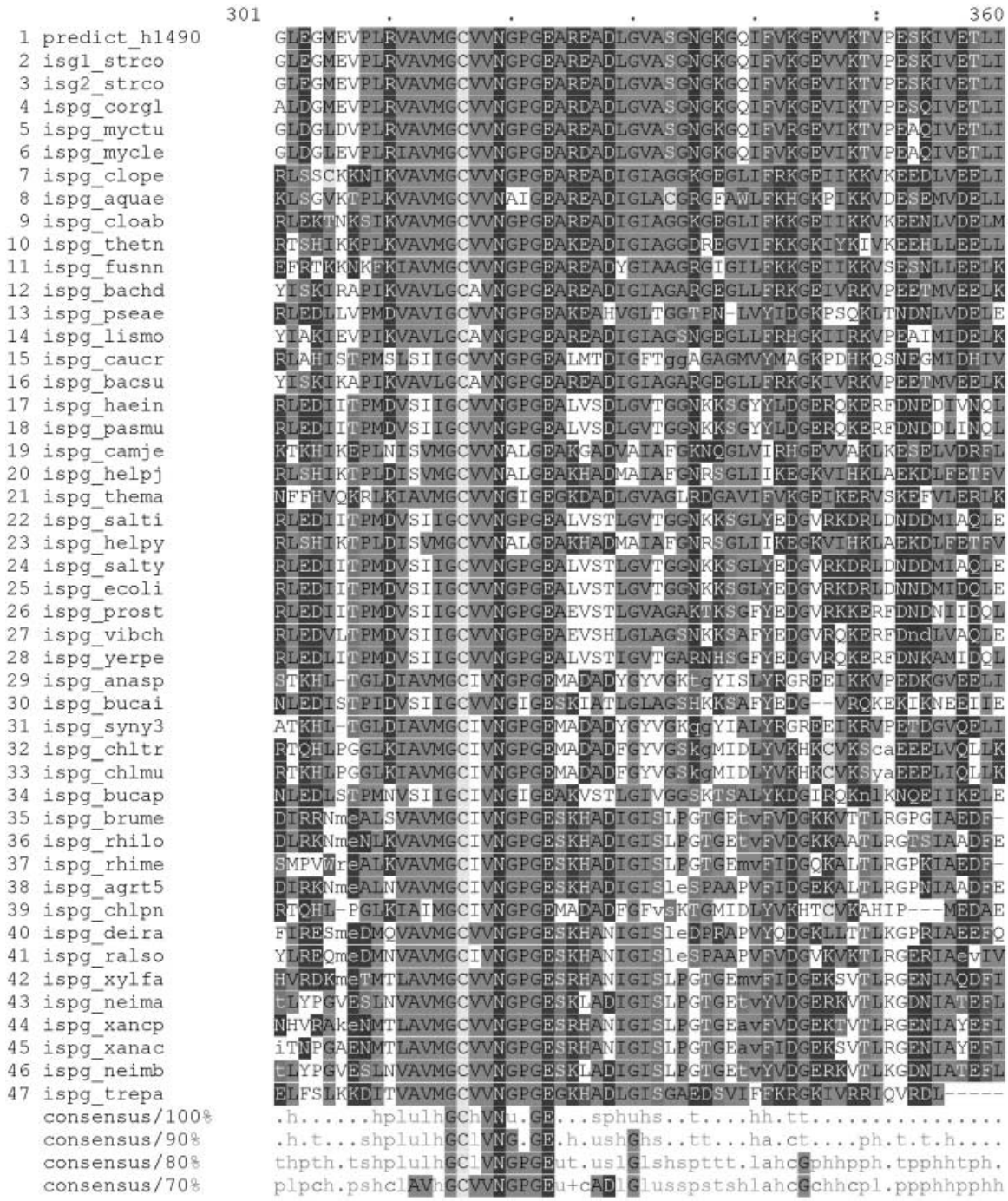

Figure 1. *(continued).*

ment,[28] and energy optimization with AMBER,[29] without the Fe_4S_4 cluster, and subsequently the TRIPOS force field[30] with the Fe_4S_4 cluster bound to the three conserved cysteine residues. The optimized structure was analyzed for stereochemical quality with PROCHECK.[31] All dihedral angles of all residues are located in most favored (66 residues = 76.7 %) and in additionally allowed regions (20 residues = 23.3 %) of the Ramachandran plot. All other criteria such as peptide bond planarity, hydrogen bond energy, etc. are within values statistically expected for proteins with a resolution below 2 Å. The quality of the final model was also checked with PROSA II. This program delivers an objective criterion as to whether the modeled protein structure is overall (or only in partial sequences) misfolded or if it represents a native folded structure.[32] The resulting plot is shown in Figure 3. There is no striking difference in the energy graph of the model structure relative to the template structure. This clearly indicates that the fold of the model has high quality and may represent a native one.


```
isg1_strco   L R Q R G L E I V S   C P S C . . . . . .   . G R A Q V D V Y K   L A E E V T A G L E
similarity   - R   + + + + + V S   + P + C               + R - + + - + + +   - + + - + + A + + +
1aop.pdb     Q R E N S M A C V S   F P T C P L A M A E   A E R F L P S F I D   N I D N L M A K H G
sec.         H H H H E E E C C C   C C C C C C C C C C   C C C H H H H H H H   H H H H H H H H H C
structure

isg1_strco   G M E V P L R V A V   M G C V V N G P G E   A R E A D L G V A S   . G N G K G Q I F V
similarity   -   + + + +   + + V   + G C +   N G + G +   A   + A + + G + + +   + + G + + + + + +
1aop.pdb     V S D E H I V M R V   T G C P . N G C G R   A M L A E V G L V G   K A P G R Y N L H L
sec.         C C C C C C C E E E   E C C C . C C C C C   H H H C C E E E E E   E E C C E E E E E E
structure

isg1_strco   K G E V . V K T V P   . . . . .   . E S   K I V E T L I E E A   M R I A E Q M E K D
similarity   + G + +   + - + + P               E     + I + + - L + E + +   R + A + + + E + +
1aop.pdb     G G N R I G T R I P   R M Y K E N I T E P   E I L A S L D E L I   G R W A K E R E A G
sec.         C C C C C C C C C C   E E E E E E E E H H   H H H H H H H H H H   H H H H H H C C C C
structure
```

Figure 2. *Alignment of the fragment L271 – A375 of GcpE of* Streptomyces coelicolor *(first row) with the fragment Q427 – G547 of a sulfite reductase of* Escherichia coli *(third row, pdb: 1AOP) and its secondary structure (fourth row).*

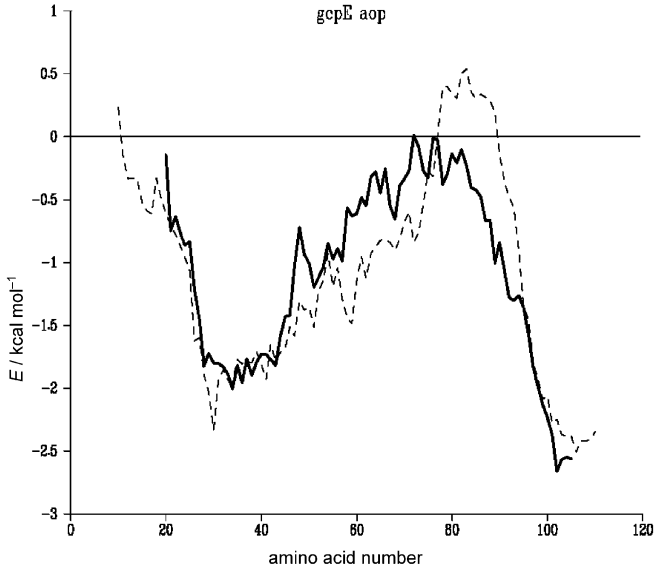

Figure 3. *Prosa Plot of the template protein fragment (1AOP); dashed lines in comparison to the model of GcpE from* Streptomyces coelicolor *(solid line).*

In addition, molecular dynamics simulations were carried out to find an optimal docking arrangement of NADPH, which has been considered to serve as a cofactor for the electron and hydrogen transfer to the ligand mediated by the Fe_4S_4 cluster. For this purpose NADPH was manually positioned in such a way that the nicotinamide moiety was close to the Fe_4S_4 cluster. Molecular dynamics simulations followed by energy optimization resulted in a surprisingly excellent docking arrangement of NADPH to the enzyme model. The amide group of the nicotinamide forms hydrogen bonds to the side chain of 100% conserved N319 and to a phosphate group of the ligand (see Figures 4 and 5, below). Strong salt bridges are formed between the second phosphate of the diphosphate group and K337 and the terminal phosphate group with K348. Furthermore, hydrophobic interactions occur between the adenine group and the side chain of V318 and of the nicotinamide with the side chain of V317. Finally, hydrogen bonds are formed between the first phosphate of the diphosphate and Q288, ad between one hydroxyl group of the first sugar residue and the backbone carbonyl group of R286. If we compare these interactions with the conserved residues shown in the multiple alignment, it is obvious that a similar interaction can also occur in all other proteins of this family. V318 is 100% conserved and in the position of V317 only hydrophobic amino acid residues such as valine, isoleucine, or alanine (the last of these in only three cases) can be detected. Lysine, arginine, or a hydrophilic amino acid residue such as serine or threonine can be found in the other related proteins close to the position of K337 in the sequence of *Streptomyces coelicolor*. Furthermore, K348 is also situated in a range in which a basic amino acid residue occurs in all enzymes. Glutamine 288 can be substituted by other hydrophilic amino acid residues which may form a hydrogen bond to a phosphate group. In known protein structures crystallized together with NADPH, similar interactions to those in our model can be observed. For instance, in a structure of GDP-fucose synthase (pdb entry 1bsv)[33] or dihydrofolate reductase (pdb entry 1df7),[34] both the nicotinamide and the adenine group exhibit hydrophobic interactions with leucine and isoleucine residues. The phosphate groups are complexed by several arginine residues. Like any docking based on a limited data set, the proposed model should be considered as a temporary solution. However, all findings strongly support the detected docking arrangement of NADPH to GcpE. Analogous simulations with $FMNH_2$ as putative ligand as suggested by Seemann et al.[12] were also performed for comparison. However, the detected interactions with the protein portion available for modeling are much weaker than those found with NADPH. Even the formation of a salt bridge of the phosphate with Lys337 cannot be formed when the flavin unit is located close to the Fe_4S_4 cluster. This result makes it very likely that NADPH will be bound in this part of the enzyme. However, $FMNH_2$ can bind to another part of the enzyme, outside of the sequence amenable for modeling, and thus $FMNH_2$ might act as electron carrier in the whole process. However, whether $FMNH_2$ or NADPH or both in succession deliver the electrons to the Fe_4S_4 cluster, has no immediate consequence for the mechanism of the reductive opening of **7** itself.

The last crucial step in the evaluation of the model was the docking of (2*S*,3*R*)-2,4-dihydroxy-3-methyl-buta-1,3-diyl-cyclodi-

phosphate (**7**) to the enzyme model. The resulting arrangement of **7** is shown in Figures 4 and 5.

It is of particular interest that MEcPP is mainly bound by three amino acid residues which are 100% conserved. In this docking, R286 forms only one hydrogen bond to MEcPP (**7**). The distance between one hydrogen atom of the guanidinium NH group and the oxygen atom linked to C3 of **7** is 2.1 Å. The special spatial docking arrangement does not allow other hydrogen bonds of this knowledge of the protein structure we cannot decide if further stabilization of the ligand enzyme complex will occur, for instance through complexation of the phosphate group by a magnesium ion and additional interactions with those parts of the protein which could not be modeled. It is very likely that such Lewis acid activation, mostly by Mg^{2+}, also takes place here. Despite these uncertainties the proposed docked conformation probably will not be changed essentially around the diphosphate group when it is additionally complexed to a magnesium ion, and therefore the mechanism discussed below should remain valid at large.

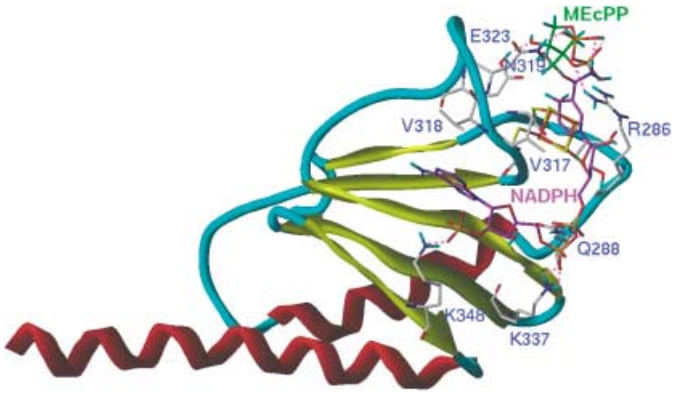

Figure 4. *The predicted secondary structure of the fragment L271 – A375 of GcpE protein of* Streptomyces coelicolor *with the active site moiety at the upper right corner. Magenta highlights carbon atoms of NADPH and green carbon atoms of the substrate MEcPP.*

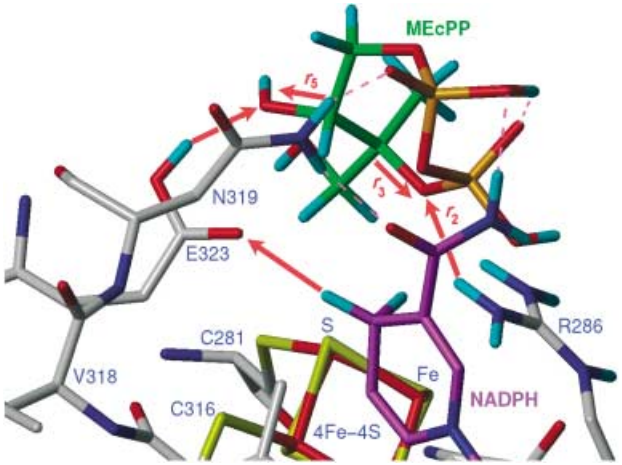

Figure 5. *Part of the active site model of GcpE protein of* Streptomyces coelicolor. *Carbon atoms in magenta highlight NADPH and green carbon atom the substrate MEcPP (N: blue, O: red, P: orange, S: yellow, Fe: red, acidic H: cyan). Red arrows label the most important steps in the enzyme catalysis. For details see Figures 6, 8, 11, and 12.*

R286 to the phosphate groups of **7**. However, we have to state that we used the neutral protonated diphosphate form in all calculations. This is supported by the semiempirical calculation discussed below, because a cleavage of the C3–O bond without passing a high energy barrier is only possible in the neutral form of MEcPP. The binding of the ligand is additionally stabilized by the formation of a hydrogen bond of the other phosphate group and the side chain of the 100% conserved N319. However, with

The interaction of the ligand with the side chain of E323 is of special interest for the catalytic mechanism. The protonated side chain of conserved E323 forms a hydrogen bond to the oxygen atom of the hydroxyl group attached to the C2 atom of MEcPP (**7**). The model clearly demonstrates the functional importance of nearly all amino acids which are 100% conserved. In particular the three cysteines that bind the Fe_4S_4 cluster; and N319, R286, and E323 which bind the ligand, and of which the last two participate in the catalysis, have to be mentioned. These results strongly support the correctness of the structure of the generated enzyme model fragment. The overall structure is shown in Figure 4, and the active site is depicted in detail in Figure 5. The quality of the model has been accepted by The Protein Data Bank[24] (entry code 1OX2) from where it can be downloaded for detailed inspection.

Catalytic mechanism

Based on these results we continued to look in more detail at the likely reaction mechanism for the opening of the cyclodiphosphate ring and the reductive abstraction of the hydroxyl group. For this purpose, a small model of the active site consisting of the substrate, R286 (using the methylguanidinium cation as a model for an arginine residue), and E323 (using acetate as a model) was created to serve in semiempirical calculations. The spatial starting arrangement of these groups was taken exactly as it was found in the enzyme model. In the first step, we investigated the energy profile for a possible proton transfer from arginine to the oxygen atom connecting the C3 atom with the phosphate group (labeled r_1 in Figure 6). The heat of formation of the

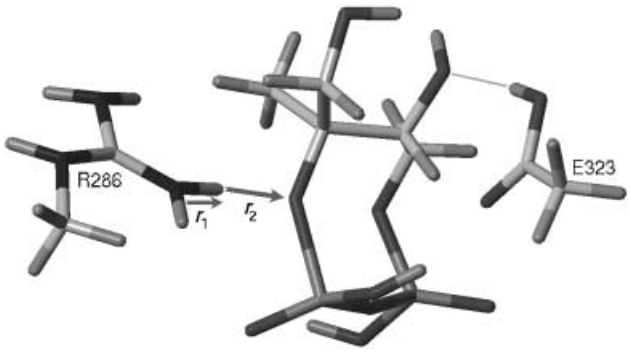

Figure 6. *The starting point model of the semiempirical PM3 reaction coordinate calculations (cf. Figure 7). The distance of the r_1-labeled N–H bond is lengthened, and simultaneously the proton moves along r_2 to bind the oxygen atom of the diphosphate ester bond of the substrate.*

optimized starting structure was calculated to be -499.4 kcal mol^{-1}. By comparison with the heats of formation of the isolated compounds (-482.6 kcal mol^{-1} as labeled in Scheme 3), an energy gain of -16.8 kcal mol^{-1} results for the formation of the complex. However, additional interactions such as with N319, which increase the affinity of the ligand to the enzyme, or to Mg^{2+} ions, are not included in the semiempirical calculations.

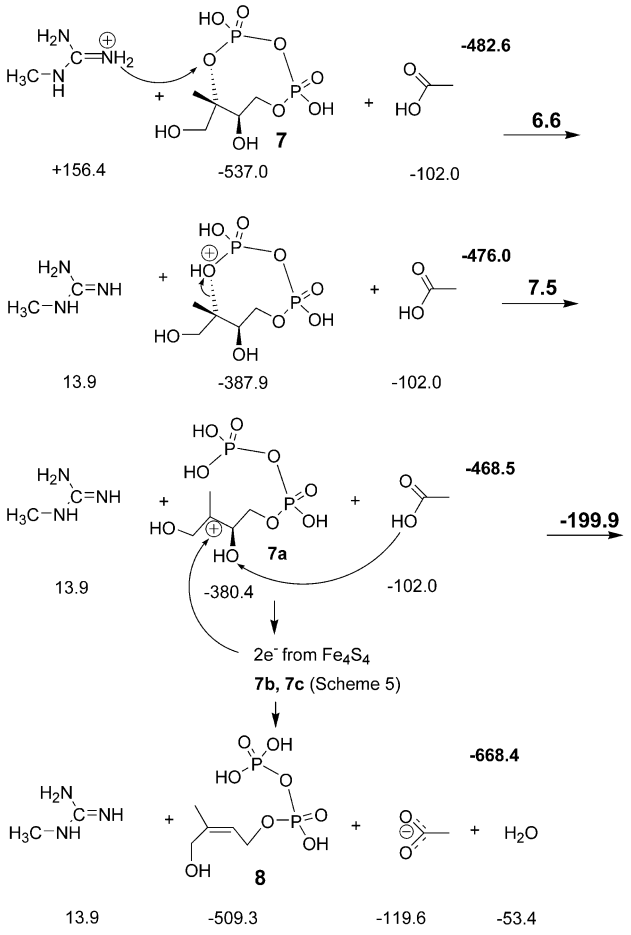

Scheme 3. *Formal mechanisms of the cleavage of the ring system of MEcPP (**7**), reduction, and hydroxyl abstraction to form HMBPP (**8**). Heats of formation and reaction enthalpies in kcal mol^{-1}; bold figure in each row is the sum of the heats of formation.*

The energy profile for the lengthening of the N–H bond of the guanidinium cation is shown in Figure 7. The proton transfer from arginine to the substrate causes an energy increase to -484.9 kcal mol^{-1} via a barrier of 24.0 kcal mol^{-1} at a distance of the proton to the oxygen atom (r_2 in Figure 6) of 1.6 Å. Next, we analyzed the cleavage of the C3–O bond (labeled with r_3 in Figure 8). Figure 9 shows the energy profile of this transformation, which leads to a further energy increase to -466.9 kcal mol^{-1} via an energy barrier of -460.3 at a C3–O distance of 2.3 Å. However, it is highly important for the next step of the mechanism that the energy of the LUMO of the complex drops down from -90.0 kcal mol^{-1} to -143.5 kcal mol^{-1} (Figure 10).

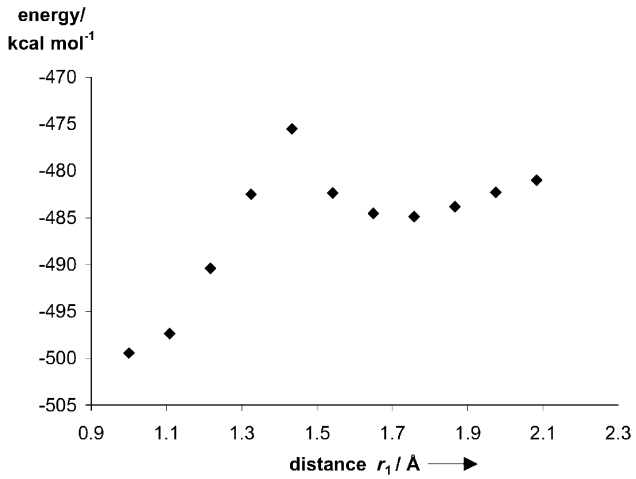

Figure 7. *Heat of formation of the complex as a function of the length of the N–H bond (r_1) of the methylguanidinium cation, and simultaneous proton transfer to the oxygen ester atom linked to C3 of the substrate (cf. Figure 4). At an N–H separation of 1.6 Å the proton is covalently bound to the oxygen atom of the substrate.*

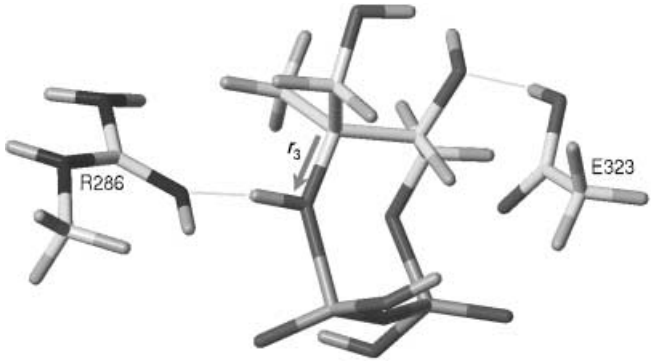

Figure 8. *Model of the second step of the reaction coordinate from semi-empirical PM3 calculations of protonated MEcPP (cf. Figures 9 and 10). The distance of the C3–O bond labeled r_3 is lengthened.*

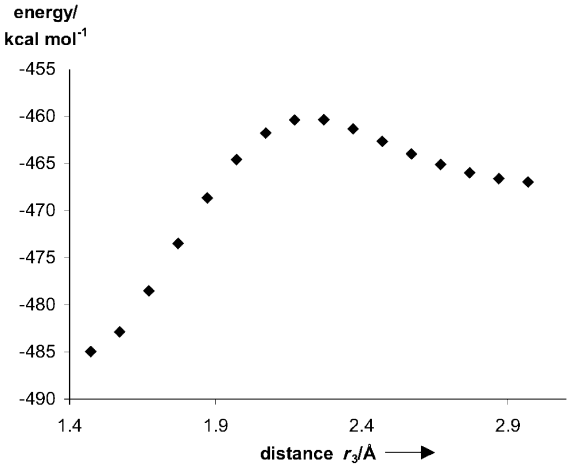

Figure 9. *Heat of formation of the complex as a function of the length of the C3–O bond (r_3) of the substrate (cf. Figure 5).*

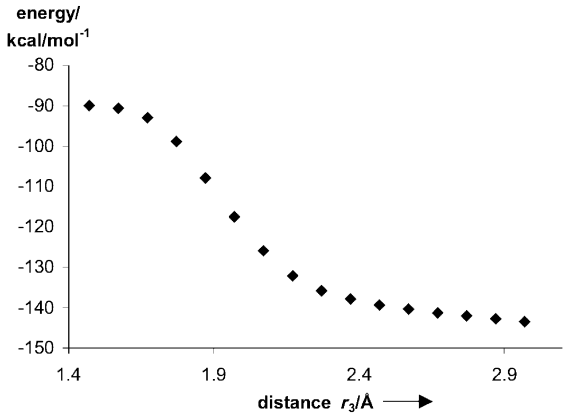

Figure 10. *LUMO energy of the complex (cf. Figure 8) as a function of the length of the C3–O bond (r_3) of the substrate (cf. Figure 5).*

Recently, Rohdich et al.[23] suggested the formation of an epoxide as an intermediate. The semiempirical calculations of both possible *O*-protonated epoxides (Scheme 4), show a further increase in the heat of formation of the complex to -453.0 kcal mol^{-1} or -453.7 kcal mol^{-1}, respectively, and of

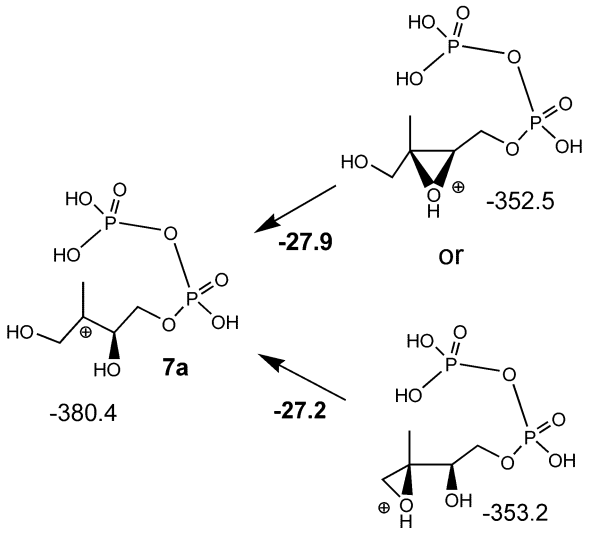

Scheme 4. *Calculated heats of formation of the epoxide intermediates suggested by Rohdich et al.[23]*

the isolated intermediates to -352.5 kcal mol^{-1} and -353.2 kcal mol^{-1} (cf. the cation **7a** shown in Scheme 3 and Scheme 4, heat of formation -380.4 kcal mol^{-1}). Furthermore, the energy of the LUMO of the formed epoxides is -84.4 kcal mol^{-1} or -103.7 kcal mol^{-1}, which is between 40 kcal mol^{-1} and more than 50 kcal mol^{-1} higher than in the former intermediate (-143.5 kcal mol^{-1}) and will significantly reduce the likelihood for the acceptance of two electrons. As seen in the optimized structure of the intermediate in the enzyme complex (Figure 11), the cation at C3, formed by elimination of the protonated diphosphate, is close (2.8 Å) to the most accessible iron atom of the Fe_4S_4 cluster, suggesting a stabilizing interaction of the iron's HOMO with the LUMO of the substrate cation **7a**. According to these results, the formation of an epoxide as an intermediate appears to be unlikely. However, such an epoxide might form if the reactive intermediate could be released from the enzyme before the subsequent reduction step.

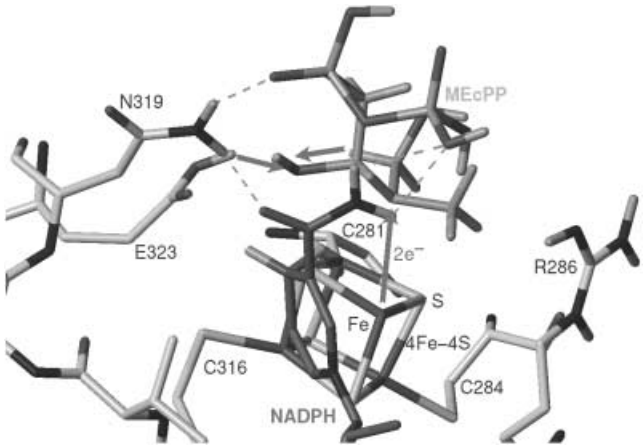

Figure 11. *Predicted docking arrangement of the intermediate "cation" in the active site of gcpE. Red arrows indicate the last steps in the catalytic mechanism.*

It is well known that Fe–S clusters function as integral components of multi-electron oxidoreductase proteins in which catalytic transformations are often accompanied by a multiple transfer of electrons, as occurs in reductases and several hydrogenases.[27, 35] DFT calculations performed for similar clusters, including molybdenum or vanadium, showed high-spin states (e.g., $S_b = 7/2$).[36] Due to insufficient parameterization of transition metals especially in high-spin states in semiempirical methods it will not make sense to include the Fe_4S_4 cluster in the calculations. It is clear from the basic chemical reaction mechanism that two electrons are needed for the reduction, but it is beyond the scope of this paper to decide in which detailed mechanism the electrons are transferred to the substrate. A stepwise two-radical transfer was suggested by Seemann et al. in 2002[12] supported by the presence of the Fe_4S_4 cluster. Probably under participation of an endogenous reduction system using $FMNH_2$ of flavodoxin, the oxidized flavodoxin cofactor will be recycled by flavodoxin reductase and NADPH. Independent from this open question, the ligand intermediate can accept electrons from the cluster owing to the very low LUMO energy of the active intermediate of the ligand and the close distance (2.8 Å) of the C3 carbocation to the "free" iron of the Fe_4S_4 cluster.

The addition of one electron to the formed carbocation (**7a**, Scheme 5) after cleavage of the C3–O bond leads to a stable neutral radical intermediate (**7b**, Scheme 5) with a considerable energy gain for the isolated ligand of -174.7 kcal mol^{-1}. Seeman et al.[12] suggested that, starting from this radical intermediate, the hydroxyl group can be removed by forming a second radical carbocation (**8a**, path **A**, Scheme 5). However, in this case the protonation of the leaving hydroxyl group would increase the heat of formation enormously to -138.6 kcal mol^{-1}, which is an energy effort of 152.9 kcal mol^{-1} to form such an intermediate

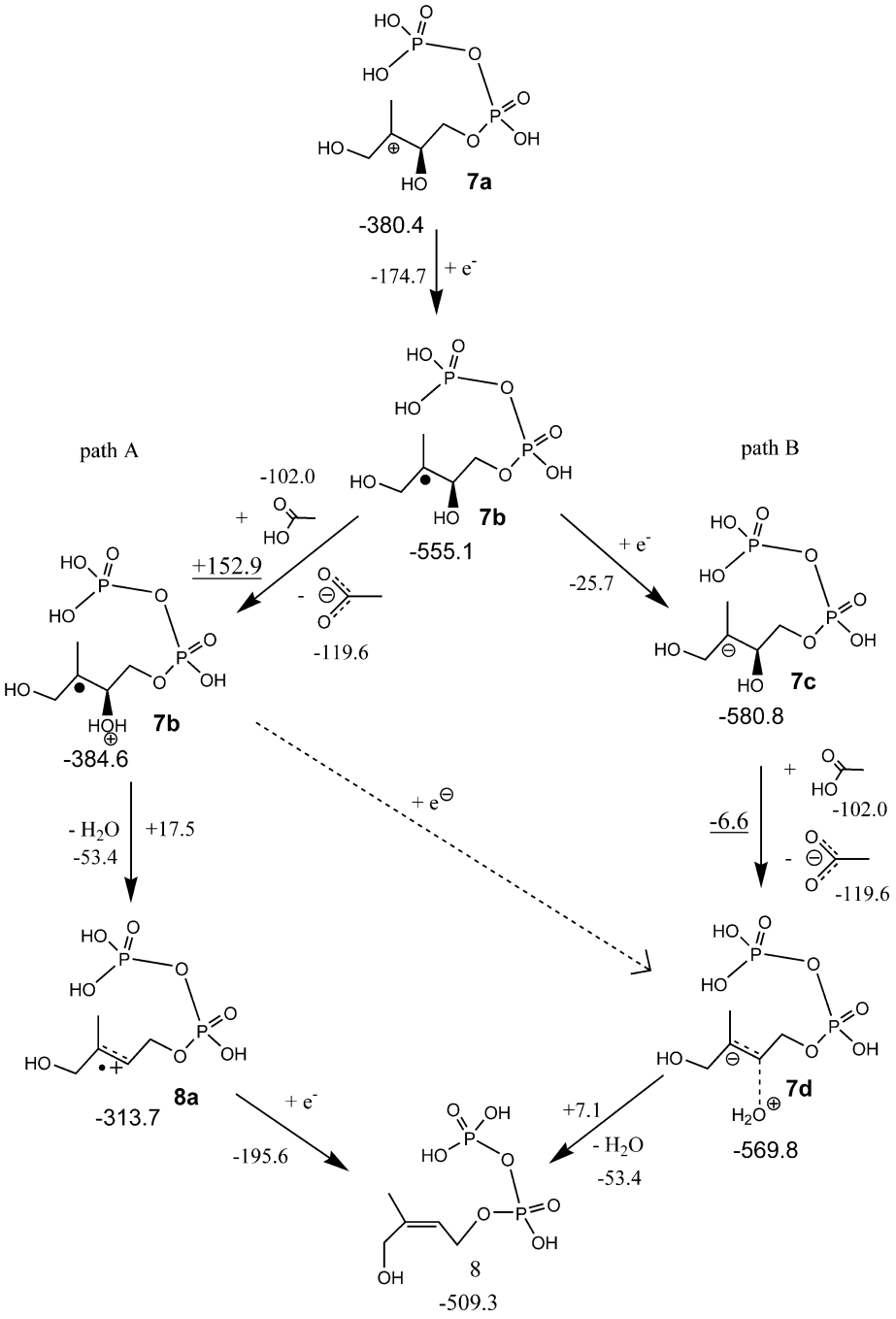

Scheme 5. *Calculated heats of formation and reaction enthalpies for the comparison of alternative pathways for the reductive formation of **8** and water. **Path A**: mechanism suggested by Seemann et al.;[12] **path B**: our proposed mechanism, highly supported by the reaction enthalpies (underlined numbers of reaction enthalpies in kcal mol^{-1}).*

7b. Furthermore, the formation of the suggested intermediate **8a** would need an additional 17.5 kcal mol^{-1}. These results clearly indicate that the abstraction of the hydroxyl group from the substrate at the state of cation radical **7b** is very unlikely. From our results it appears much more likely that two electrons are transferred to the carbocation intermediate **7a** to form the corresponding anion **7c** (either stepwise by intermediate recovery of the electron configuration of the Fe_4S_4 cluster or by immediate two-electron transfer under participation of NADPH and/or $FMNH_2$ as an electron delivery system, Scheme 5).

The addition of a second electron to the aforementioned neutral radical **7b** leads to a further energy gain of 25.7 kcal mol^{-1}, which highly supports the formation of this anion intermediate. The formation of such a carbanion-like species would of course coincide with the protonation of the 2-hydroxy group and subsequent elimination of water. This is proved by the addition of one proton to the intermediate anion **7c** (path **B**, Scheme 5), which leads to immediate fragmentation and the formation of the final product complexed with water (**7d**, Scheme 5). The energy effort of 7.1 kcal mol^{-1} for the formal complete cleavage of the complex into **8** and water just indicates noncovalent attractive interactions between water and the final product **8**.

To study the final step of the conversion of **7** to **8** within the whole system according to Scheme 3, we studied the energy profile of the proton transfer of acetic acid (labeled r_4 in Figure 12) to the leaving hydroxyl group of the substrate anion **7c**. For this transfer a low energy barrier of 13.6 kcal mol^{-1} must be overcome to give the final product, including again spontaneous cleavage of the hydroxyl group and the formation of water. Expectedly, this process provides a considerable energy gain of approximately 200 kcal mol^{-1} (Scheme 3) when the energy gain by addition of two electrons is included, which strongly supports the proposed mechanism. The resulting complex consists of the product HMBPP (**8**), water, acetic acid anion (as a mimic for E323), and the neutral methylguanidine (for R286, Figure 13). The resulting formal energy gain, taking into account only the heats of formation of the isolated compounds for the whole process, is approximately 186 kcal mol^{-1} (cf. Scheme 3). However, this huge energy gain is somewhat misleading, since two electrons, delivered either from $FMNH_2$ and/or NADPH by oxidation of these compounds, have been added to the system during the conversion. This electron injection requires some energy. Nevertheless, if for the instance the nicotinamide form of NADPH (as a two-proton and a two-

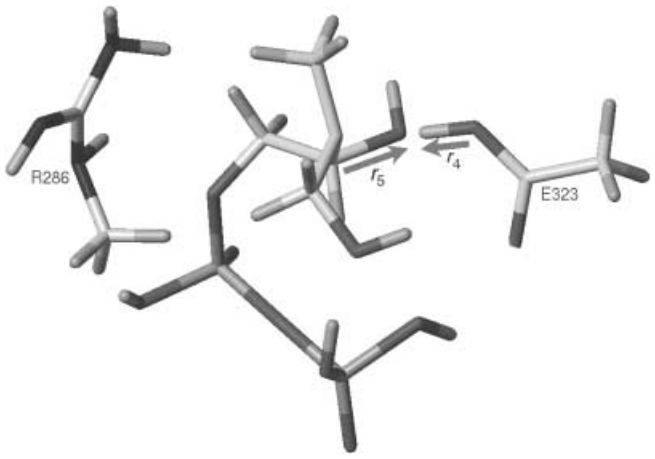

Figure 12. *The last step of the semiempirical PM3 reaction coordinate calculations (Figure 13). The distance of the r_4-labeled acid O–H bond is lengthened. With the attack of the proton at the 2-hydroxy group of the ligand, the C2–O bond (r_5) is spontaneously cleaved.*

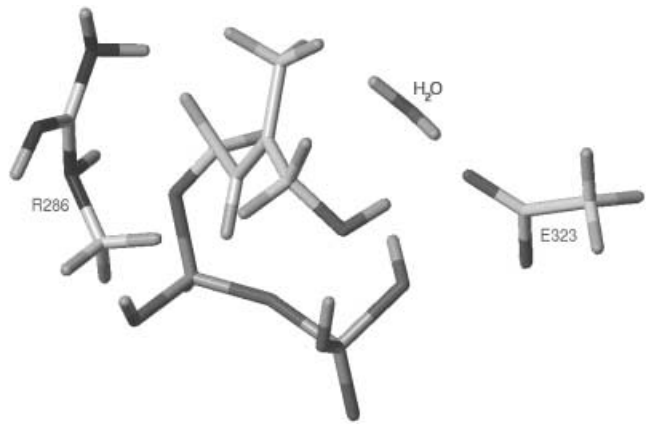

Figure 13. *Suggested structure of the final complex with formed HMBPP and water.*

electron delivery system) is included and the reprotonation of the acetic acid anion is considered, the whole process is still thermodynamically favored by some 3 kcal mol^{-1}. Additional gains may result from an altered Mg^{2+} binding of the now unconstrained diphosphate moiety.

Discussion

We have developed a model of the fragment L271 – A375 of the GcpE protein of *Streptomyces coelicolor* (Swissprot: Q9X7W2)[18] as a representative example for all enzymes of the *GcpE* (*ispG*) family. This model includes the most important binding areas of the Fe_4S_4 cluster and a probable one of NADPH, and the substrate. It can be assumed that additional amino acid residues, which are not included in the fragment covered here, will take part in the binding of the ligand through the diphosphate group, and thus will enhance the docking affinity even more than was shown in the presented model. These residues can either be basic, such as arginine or lysine (cf. pdb entry 1df7),[34] or alternatively acidic residues, which complex divalent cations. Unfortunately, as a result of missing homology to any other protein with known X-ray structure, it was not possible to model further fragments of the enzyme, and such a truncated model as the one presented here has to be considered with the necessary caution. The energy gain expected for the docking of the substrate in the enzyme's active site can be assumed to account for the approximate 17 kcal mol^{-1} required to overcome the thermodynamically disfavored barrier for the first two steps in the catalytic mechanism (cf. Scheme 3). The reaction enthalpy for the whole reaction sequence is some -186 kcal mol^{-1}, not including efforts for the oxidation of any electron delivery system, but also excluding energy gains from solvation of the product upon its release. Additionally, the cleavage of the MEcPP ring system to form HMBPP and water leads to an increase of the entropy of the whole system. Thus, both the enthalpy and the entropy contribute to a thermodynamically favorable process thereby supporting the proposed mechanism.

In light of these results, other proposed mechanisms,[12, 23] which include radical intermediates in the conversion process, appear less likely. Radical intermediates will nevertheless have to be taken into account (e.g., **7b**, Scheme 4). However, here it could be demonstrated that the dehydration of **7** is only favored once the ligand has accepted two electrons to form an intermediate anion **7c** but is unlikely to be formed from the protonated radical to give a radical cation **8a** as suggested by Seemann et al.[12] Furthermore, as discussed before, the formation of an epoxide intermediate also appears unlikely in this model, because this intermediate would cause a considerable increase of the heat of formation. In addition, the very likely interaction of the carbocation at C3 with the iron cluster in the enzyme and of the hydroxyl group at C2 with E323, as seen in Figure 11, would be hampered in the epoxides.

Altogether the proposed mechanism is consistent with the model of a partial sequence of the enzyme, but especially with the thermodynamic and kinetic calculations (activation barriers are low) and the experimental results of us and others.

The conversion of HMBPP (**8**) to IPP (**9**) and DMAPP (**10**) is the last step in the DXP pathway. It also constitutes a reductive dehydroxylation, in principle not unlike that of the previous step. Also, the experimental and sequence data of the enzymes involved (*ispH*/*LytB*) suggest this (e.g., see ref. [37]). Thus we analyzed the sequence of *LytB* protein concerning conserved amino acid residues to find homologues with known X-ray structure. It appeared that, similarly to *GcpE*, the family of *LytB* enzymes also contains three conserved cysteine residues, which is an indication that an Fe_4S_4 cluster is bound to these residues in a similar fashion as reported above. However, no homology was found to any other protein with known three-dimensional structure, even if smaller fragments were considered in a procedure similar to that applied for *GcpE*. Nevertheless, a mechanism analogous to that discussed above may be assumed for the final step of the DXP pathway. A speculative mechanism would involve a 2,4-allylic cation formed by hydroxide abstraction after protonation, and the subsequent or simultaneous

delivery of two electrons supported by the Fe_4S_4 cluster followed by protonation of the allylic system either in the 2-position to yield IPP, or in the 4-position to yield DMAPP. However, such a site-unspecific hydrogenation is not necessarily to be expected from an enzyme. Another, also somewhat speculative conclusion can be drawn if the heats of formations of IPP (**9**) and DMAPP (**10**) are compared. The PM3-optimized structures gave a heat of formation of -469.7 kcal mol^{-1} for IPP but a heat of formation of -474.4 kcal mol^{-1} for DMAPP. The higher stability of DMAPP also offers the chance for a nonenzymatic or at least nonspecific conversion of IPP to DMAPP. In this case, by means of LytB, IPP is formed initially, which then partially isomerizes to the thermodynamically more stable DMAPP, for example, by general acid catalysis in, at, or less likely outside the active site. The exact nature of the mechanism of the seemingly simultaneous (?) formation of the two final products[22] in the last step of the DXP/MEP pathway will remain an open question until more detailed structural and mechanistic data become available.

Experimental Section

Synthesis of [4-^{2}H](*E*)-3-methyl-4-oxobut-2-enyl diphosphoric acid (12 b): *o*-Iodoxybenzoic acid (IBX, 92 mg, 328 μmol) was added to a suspension of (*E*)-4-hydroxy-3-methylbut-2-enyl diphosphate (**11 b**, 21.6 mg, 82 μmol)[17] in dry dimethyl sulfoxide (DMSO, 1.1 mL). The mixture was stirred at room temperature (25 °C). After 4 h, the reaction mixture was cooled to 0 °C and $NaHCO_3$ (27.5 mg, 328 μmol) in water (4 mL) was added. The solvent mixture was removed in vacuo and the evaporation residue was dissolved in water (1.5 mL). The resulting solution was applied to a DEAE Sephadex column (formate-form, 1.0×18 cm) which was eluted with water with a linear gradient of 0.06 M to 0.56 M ammonium formate, pH 8.0 at a flow rate of 1.1 mL min^{-1}. The retention volume of the aldehyde was 200 mL. The fractions containing the aldehyde were combined and applied to 20 mL Dowex 50w $\times$ 8 resin (H^+ form). The acidic eluate was collected and evaporated under reduced pressure almost to dryness. Then, water (5 mL) was added and evaporated again to yield the oily aldehyde (14.2 mg, 10:7 mixture of ^{2}H-labeled (**12 b**) and unlabeled (**12 a**) compound). The total yield for the ^{2}H-labeled compound was 30%. ^{1}H NMR (400 MHz, D_2O) **12 a**,**b**: $\delta = 9.37$ (s, 0.5 H; H-1), 6.81 (t, $J = 5$ Hz, 1 H; H-3), 4.86 (m, 2 H; H-4), 1.74 ppm (s, 3 H; CH_3); Negative mode MS (ESI): *m/z* (%) **12 b**: 260 $[M-H]^-$ (100), 242 $[M-H-H_2O]^-$; *m/z* (%) **12 a**: 259 $[M-H]^-$ (72), 241 $[M-H-H_2O]^-$, 177 $[H_3P_2O_7^-]$, 159 $[HP_2O_6^-]$, 97 $[H_2PO_4^-]$, 79 $[PO_3^-]$.

Synthesis of [4-^{3}H](*E*)-3-methyl-4-oxobut-2-enyl diphosphoric acid (12 c): [4-^{3}H](*E*)-4-hydroxy-3-methylbut-2-enyl diphosphate (**11 c**, 74 μCi, specific activity: 1.56 μCi nmol^{-1}[17]) was oxidized with IBX (2.6 mg, 9.3 μmol), isolated, and purified as described above to give the corresponding tritiated aldehyde (**12 c**, 22.2 μCi, calculated specific activity: 0.78 μCi nmol^{-1}) in 30% yield.

Isolation of chromoplasts from *Capsicum annuum*: Isolation of chromoplasts from *C. annuum*, incorporation experiments with isotope-labeled substrates, isolation of phytoene, and HPLC analyses of phosphorylated metabolites were conducted exactly as previously published.[17]

Enzyme assay 1: Reaction mixtures of 200 μL total volume contained Hepes buffer (100 mmol pH 7.6), NaF (5 mmol), adenosine monophosphate (1 mmol), NADPH (2 mmol), NADH (2 mmol), unlabeled (*E*)-4-hydroxy-3-methylbut-2-enyl diphosphate (**11 a**, 50 μmol), [4-^{3}H](*E*)-4-hydroxy-3-methylbut-2-enyl diphosphate (**11 c**, 3.2 μmol), and chromoplasts of *C. annuum* (0.2 mg). Reference reaction mixtures of 200 μL total volume contained Hepes buffer (100 mmol pH 7.6), NaF (5 mmol), adenosine monophosphate (1 mmol), NADPH (2 mmol), NADH (2 mmol), unlabeled (*E*)-3-methyl-4-oxobut-2-enyl diphosphoric acid (**12 a**, 50 μmol), [4-^{3}H](*E*)-3-methyl-4-oxobut-2-enyl diphosphoric acid (**12 c**, 1.6 μmol), and chromoplasts of *C. annuum* (0.2 mg).

Enzyme assay 2: Reaction mixtures of 100 μL total volume contained Tris-HCl buffer (100 mmol pH 8.0), NaF (3.5 mmol), adenosine monophosphate (1 mmol), [4-^{3}H] (*E*)-4-hydroxy-3-methylbut-2-enyl diphosphate (**11 c**, 3.2 μmol) and Tzs protein (0.5 μg) from *Agrobacterium tumefaciens* C58. Reference reaction mixtures of 100 μL total volume contained Tris-HCl buffer (100 mmol, pH 8.0), NaF (3.5 mmol), adenosine monophosphate (1 mmol), [4-^{3}H](*E*)-3-methyl-4-oxobut-2-enyl diphosphoric acid (**12 c**, 1.6 μmol), and Tzs protein (0.5 μg) from *Agrobacterium tumefaciens* C58.

Computational methods: Sequences of all available GcpE enzymes were aligned and their secondary structures were predicted by using PHDsec.[38–41] The conserved amino acid residues were identified (Figure 1).

We tried to find homologous proteins with known three-dimensional structure (X-ray or NMR). For this purpose 3D-pssm was used.[25, 26] The sequence of *Streptomyces coelicolor* (Swissprot: Q9X7W2)[18] was chosen as a representative member for all enzymes of this family. However, no proteins with sufficiently high homology allowing the application of homology modeling techniques were obtained. Subsequently the template sequence was shortened at the N-terminal and C-terminal regions of the sequences by focusing on the likely active site surrounded by the three conserved cysteine residues (cf. Figure 1). Finally, for fragment L271 – A375 we obtained a sequence identity with a score of 25% and an PSSM-E-value of 1.66×10^{-8} homology with a sulfite reductase of *Escherichia coli* (pdb: 1AOP)[27] with more than 95% certainty to be useful for homology modeling. MOE (molecular operating environment, Chemical Computing Group Inc.) was used for homology modeling of the partial sequence of *Streptomyces coelicolor*.[18] The sequences were aligned by using the blosum62-matrix (Figure 2).[42, 43]

Ten models were calculated by MOE and pre-optimized by using the AMBER94 force field.[29] All ten models were checked with regard to stereochemical quality using PROCHECK.[31] The best one was used for further refinement. Finally, the structure of the Fe_4S_4 cluster was taken from the X-ray-structure of the aforementioned sulfite reductase and manually docked close to the three conserved cysteine residues, which were considered to bind the cluster covalently. The complete model thus obtained was refined by using the TRIPOS force field[30] and Gasteiger charges,[44] which are implemented in the SYBYL molecular modeling package[45] for Silicon Graphics workstations. Possible docking arrangements of $FMNH_2$ and NADPH were investigated by molecular dynamics simulations.[3] The backbone atoms of the enzyme were fixed and the dynamics simulation was performed for 20000 fs by using a nonbonded cut-off of 16 Å; we investigated the subsequent minimization. Surprisingly, an excellent docking arrangement of NADPH to the enzyme was obtained without any changes in the backbone dihedral angles of the enzyme. By using the same procedure, the substrate was added to the model close to the Fe_4S_4 cluster. The quality of the final model was analyzed with PROCHECK and PROSA II (Figure 3).[32]

Semiempirical calculations were performed by using the PM3 method[46] as implemented in SPARTAN[47] to study possible reaction mechanisms and to calculate the heats of formation and reaction

enthalpies. The distance between the methyl groups of methylguanidine and acetic acid was fixed in all calculations at 9.2 Å to at least partially mimic the restrictions of translational degrees of freedom caused by the enzyme.

Keywords: DXP/MEP pathway · GcpE · homology modeling · isoprenoids · labeling studies · semiempirical calculations

[1] F. Rohdich, J. Wungsintaweekul, M. Fellermeier, S. Sagner, S. Herz, K. Kis, W. Eisenreich, A. Bacher, M. H. Zenk, *Proc. Natl. Acad. Sci. USA* **1999**, *96*, 11 758 – 11 763.
[2] F. Rohdich, K. Kis, A. Bacher, W. Eisenreich, *Curr. Opin. Chem. Biol.* **2001**, *5*, 535 – 540.
[3] F. Rohdich, S. Hecht, K. Gartner, P. Adam, C. Krieger, S. Amslinger, D. Arigoni, A. Bacher, W. Eisenreich, *Proc. Natl. Acad. Sci. USA* **2002**, *99*, 1158 – 1163.
[4] H. Lüttgen, F. Rohdich, S. Herz, J. Wungsintaweekul, S. Hecht, C. A. Schuhr, M. Fellermeier, S. Sagner, M. H. Zenk, A. Bacher, *Proc. Natl. Acad. Sci. USA* **2000**, *967*, 1062 – 1067.
[5] S. Herz, J. Wungsintaweekul, C. A. Schuhr, S. Hecht, H. Lüttgen, S. Sagner, M. Fellermeier, W. Eisenreich, M. H. Zenk, A. Bacher, F. Rohdich, *Proc. Natl. Acad. Sci. USA* **2000**, *97*, 2486 – 2490.
[6] S. Takahashi, T. Kuzuyama, H. Watanabe, H. Seto, *Proc. Natl. Acad. Sci. USA* **1998**, *95*, 9879 – 9884.
[7] K. Reuter, S. Sanderbrand, H. Jomaa, J. Wiesner, I. Steinbrecher, E. Beck, M. Hintz, G. Klebe, M. T. Stubbs, *J. Biol. Chem.* **2002**, *277*, 5378 – 5384.
[8] L. E. Kemp, C. S. Bond, W. N. Hunter, *Proc. Natl. Acad. Sci. USA* **2003**, *99*, 6591 – 6596.
[9] J. M. Estevez, A. Cantero, A. Reindl, S. Reichler, P. Leon, *J. Biol. Chem.* **2001**, *276*, 22 901 – 22 909.
[10] T. Radykewicz, F. Rohdich, J. Wungsintaweekul, S. Herz, K. Kis, W. Eisenreich, A. Bacher, M. H. Zenk, D. Arigoni, *FEBS Lett.* **2000**, *465*, 157 – 160.
[11] S. Hecht, W. Eisenreich, P. Adam, S. Amslinger, K. Kis, A. Bacher, D. Arigoni, F. Rohdich, *Proc. Natl. Acad. Sci. USA* **2001**, *98*, 14 837 – 14 842.
[12] M. Seemann, B. T. Bui, M. Wolff, D. Tritsch, N. Campos, A. Boronat, A. Marquet, M. Rohmer, *Angew Chem.* **2002**, *114*, 4513 – 4515; *Angew Chem. Int. Ed. Engl.* **2002**, *41*, 4337 – 4339.
[13] M. Hintz, A. Reichenberg, B. Altincicek, U. Bahr, R. M. Gschwind, A. K. Kollas, E. Beck, J. Wiesner, M. Eberl, H. Jomaa, *FEBS Lett.* **2001**, *509*, 317 – 322.
[14] B. Altincicek, E. C. Duin, A. Reichenberg, R. Hedderich, A. K. Kollas, M. Hintz, S. Wagner, J. Wiesner, E. Beck, H. Jomaa, *FEBS Lett.* **2002**, *532*, 437 – 440.
[15] A.-K. Kollas, E. C. Duin, M. Eberl, B. Altincicek, M. Hintz, A. Reichenberg, D. Henschker, A. Henne, I. Steinbrecher, D. N. Ostrovsky, H. Hedderich, E. Beck, H. Jomaa, J. Wiesner, *FEBS Lett.* **2002**, *532*, 432 – 436.
[16] M. Fellermeier, M. Raschke, S. Sagner, J. Wungsintaweekul, C. A. Schuhr, S. Hecht, K. Kis, T. Radykewicz, P. Adam, F. Rohdich, W. Eisenreich, A. Bacher, D. Arigoni, M. H. Zenk, *Eur. J. Biochem.* **2001**, *268*, 6302 – 6310.
[17] W. Gao, R. Loeser, M. Raschke, M. A. Dessoy, M. Fulhorst, H. Alpermann, L. A. Wessjohann, M. H. Zenk, *Angew. Chem.* **2002**, *114*, 2716 – 2719; *Angew. Chem. Int. Ed.* **2002**, *41*, 2604 – 2607.
[18] S. D. Bentley, K. F. Chater, A.-M. Cerdeno-Tarraga, G. L. Challis, N. R. Thomson, K. D. James, D. E. Harris, M. A. Quail, H. Kieser, D. Harper, A. Bateman, S. Brown, G. Chandra, C. W. Chen, M. Collins, A. Cronin, A. Fraser, A. Goble, J. Hidalgo, T. Hornsby, S. Howarth, C.-H. Huang, T. Kieser, L. Larke, L. Murphy, K. Oliver, S. O'Neil, E. Rabbinowitsch, M. A. Rajandream, K. Rutherford, S. Rutter, K. Seeger, D. Saunders, S. Sharp, R. Squares, S. Squares, K. Taylor, T. Warren, A. Wietzorrek, J. Woodward, B. G. Barrell, J. Parkhill, D. A. Hopwood, *Nature* **2002**, *417*, 141 – 147.
[19] D. B. Dess, J. C. Martin, *J. Org. Chem.* **1983**, *48*, 4155 – 4156.
[20] M. Frigerio, M. Santagostino, *Tetrahedron Lett.* **1994**, *36*, 8019 – 8022.
[21] K. Surendra, N. S. Krishnaveni, M. A. Reddy, Y. V. D. Nageswar, K. R. Rao, *J. Org. Chem.* **2003**, *68*, 2058 – 2059.
[22] M. Wolff, M. Seemann, B. Tse Sum Bui, Y. Frapart, D. Tritsch, A. G. Estrabot, M. Rodriguez-Concepcion, A. Boronat, A. Marquet, M. Rohmer, *FEBS Lett.* **2003**, *541*, 115 – 120.
[23] F. Rohdich, F. Zepeck, P. Adam, S. Hecht, J. Kaiser, R. Laupitz, T. Grawert, S. Amslinger, W. Eisenreich, A. Bacher, D. Arigoni, *Proc. Natl. Acad. Sci. USA* **2003**, *100*, 1586 – 1591.
[24] H. M. Berman, J. Westbrook, Z. Feng, G. Gilliland, T. N. Bhat, H. Weissig, I. N. Shindyalov, P. E. Bourne, *Nucleic Acids Res.* **2000**, *28*, 235 – 242.
[25] D. Fischer, C. Barret, K. Bryson, A. Elofsson, A. Godzik, D. Jones, K. J. Karplus, L. A. Kelley, R. M. Maccallum, K. Pawowski, B. Rost, L. Rychlewski, M. J. Sternberg, *Proteins* **1999**, *Suppl. 3*, 209 – 217.
[26] L. A. Kelley, R. M. MacCallum, M. J. E. Sternberg, *J. Mol. Biol.* **2000**, *299*, 499 – 520.
[27] B. R. Crane, L. M. Siegel, E. D. Getzoff, *Science* **1995**, *270*, 56 – 67.
[28] M. Chemical Computing Group Inc., Montréal, PQ, Canada.
[29] W. D. Cornell, P. Cieplak, C. I. Bayly, I. R. Gould, K. M. J. Merz, D. M. Ferguson, D. C. Spellmeyer, T. Fox, J. W. Caldwell, P. A. Kollman, *J. Am. Chem. Soc.* **1995**, *117*, 5179 – 5197.
[30] M. Clark, R. D. Cramer, III, N. J. Van Opdenbosch, *J. Comput. Chem.* **1989**, *10*, 982 – 1012.
[31] R. A. Laskowski, M. W. MacArthur, D. S. Moss, J. M. Thornton, *J. Appl. Cryst.* **1993**, *26*, 283 – 291.
[32] M. J. Sippl, *J. Comput. Aided Mol. Des.* **1993**, *7*, 473 – 501.
[33] W. S. Somers, M. L. Stahl, F. X. Sullivan, *Structure* **1998**, *6*, 1601 – 1612.
[34] R. Li, R. Sirawaraporn, P. Chitnumsub, W. Sirawaraporn, J. Wooden, F. Athappilly, S. Turley, W. G. Hol, *J. Mol. Biol.* **2000**, *295*, 307 – 323.
[35] B. R. Crane, E. D. Getzoff, *Curr. Opin. Struct. Biol.* **1996**, *6*, 744 – 756.
[36] T. Lovell, J. Li, T. Liu, D. A. Case, L. Noodleman, *J. Am. Chem. Soc.* **2001**, *123*, 12 392 – 12 410.
[37] S. D. Bentley, K. F. Chater, A. M. Cerdeno-Tarraga, G. L. Challis, N. R. Thomson, K. D. James, D. E. Harris, M. A. Quail, H. Kieser, D. Harper, A. Bateman, S. Brown, G. Chandra, C. W. Chen, M. Collins, A. Cronin, A. Fraser, A. Goble, J. Hidalgo, T. Hornsby, S. Howarth, C. H. Huang, T. Kieser, L. Larke, L. Murphy, K. Oliver, S. O'Neil, E. Rabbinowitsch, M. A. Rajandream, K. Rutherford, S. Rutter, K. Seeger, D. Saunders, S. Sharp, R. Squares, S. Squares, K. Taylor, T. Warren, A. Wietzorrek, J. Woodward, B. G. Barrell, J. Parkhill, D. A. Hopwood, *Nature* **2002**, *417*, 141 – 147.
[38] B. Rost, C. Sander, *J. Mol. Biol.* **1993**, *232*, 584 – 599.
[39] B. Rost, C. Sander, *Proteins* **1994**, *19*, 55 – 77.
[40] B. Rost, *Methods Enzymol.* **1996**, *266*, 525 – 539.
[41] C. Sander, R. Schneider, *Proteins* **1991**, *9*, 56 – 68.
[42] S. Henikoff, J. G. Henikoff, *Proc. Natl. Acad. Sci. USA* **1992**, *89*, 10 915 – 10 919.
[43] S. Henikoff, J. G. Henikoff, *Proteins* **1993**, *17*, 49 – 61.
[44] J. Gasteiger, M. Marsili, *Tetrahedron* **1980**, *36*, 3219 – 3222.
[45] TRIPOS Associates Inc., St. Louis, MO (USA).
[46] J. J. P. Stewart, *J. Comput. Chem.* **1989**, *10*, 221 – 264.
[47] Schrödinger, Inc., Portland, OR, USA, **1999**.

Received: August 15, 2003 [F 743]

